ELSEVIER

Journal of Chromatography B, 754 (2001) 345–356

JOURNAL OF CHROMATOGRAPHY B

www.elsevier.com/locate/chromb

Utilization of the non-covalent fluorescent dye, NanoOrange, as a potential clinical diagnostic tool
Nanomolar human serum albumin quantitation

M.D. Harvey, V. Bablekis, P.R. Banks, C.D. Skinner*

Department of Chemistry and Biochemistry, Concordia University, 1455 de Maisonneuve Boulevard W., Montreal, QC, Canada

Received 11 September 2000; received in revised form 30 November 2000; accepted 12 December 2000

Abstract

The commercially available dye, NanoOrange, has been investigated as a potential tool for clinical diagnostics due to its low cost, ease of use, and ability to detect nanomolar concentrations of protein. Virtually non-fluorescent in dilute aqueous solutions, NanoOrange fluorescence is enhanced by at least an order of magnitude upon non-covalent interaction with proteins. These features, coupled with the requirement for high throughput assays in the clinical laboratory has prompted the development of two orthogonal NanoOrange approaches. Human serum albumin (HSA) was used as a model protein for the development of both 96-well microplate and capillary electrophoresis laser-induced fluorescence (CE–LIF) assay formats. Dye performance in five commonly used buffers of various concentrations and pH indicated considerable flexibility in assay buffer selection, with optimal performance at pH 9.0. A salt concentration study indicated that increasing NaCl concentration generally decreases fluorescence emission and can be minimized by pre-diluting biological samples to a final salt concentration of 20–80 m*M*. Titration of protein with NanoOrange resulted in optimal HSA–NanoOrange complex formation utilizing 1× and 2× NanoOrange in the 96-well microplate and CE–LIF approaches, respectively. A NanoOrange binding model based on rapid signal enhancement and zero order fluorescence emission kinetics is proposed. The utilization of NanoOrange in CE–LIF based human serum analysis results in a signal-to-background ratio improvement of up to two orders of magnitude.

Keywords: Clinical diagnostics; Capillary electrophoresis; NanoOrange; Human serum albumin

1. Introduction

The trend towards rapid analyses in the clinical laboratory has fueled the development of commercially available high throughput analytical instrumentation. Capillary electrophoresis (CE) has gained increased acceptance as a powerful tool in clinical diagnostics, with the advent of commercially available eight capillary instrumentation capable of sampling from 96-well microplates [1–4]. This acceptance has also been dependent on advances in optical detection techniques such as laser-induced fluorescence, which have allowed for capillary electrophoretic protein analysis in the subnanomolar range [5–8]. This in turn has required the development of rapid, effective fluorescent derivatization approaches.

Covalent and non-covalent fluorescent labeling strategies have been utilized in numerous clinical CE

*Corresponding author. Tel.: +1-51-4848-7558; fax: +1-51-4848-2868.

E-mail address: cskinner@alcor.concordia.ca (C.D. Skinner).

0378-4347/01/$ – see front matter
PII: S0378-4347(00)00627-7

analyses [9–12]. Covalent labeling reagents such as fluorescein isothiocyanate, tetramethylrhodamine succinimidyl ester, and CBQCA target specific functional groups such as primary amines. The extent of conjugation is thus dependent on the number and accessibility of the respective reactive functional groups [13]. In contrast, non-covalent fluorescent probes have received increased attention in CE, particularly with respect to DNA analysis [14,15]. Non-covalent probes such as Sypro Red and Indocyanine green have been utilized effectively in subnanomolar protein analysis in a capillary format [16,17]. These dyes are believed to bind rapidly with their protein targets via electrostatic and/or hydrophobic interactions, and often do not require the same degree of reaction condition stringency typically required in covalent labeling approaches. The ideal non-covalent probe is simple to use, binds rapidly to its target, is fluorogenic, sensitive, and economical.

These features are satisfied by the relatively new commercially available dye NanoOrange. The unique chemistry of this dye is currently applied to the accurate detection of proteins in solution at concentrations between 10 ng/ml and 10 μg/ml [18]. Highly soluble and virtually non-fluorescent in aqueous solutions, NanoOrange fluorescence is dramatically increased upon protein binding. Bound dye is efficiently excited with the 488 nm line of a relatively inexpensive air-cooled Ar^+ laser, and possesses a large Stokes' shift with maximum emission at about 580 nm. Furthermore, NanoOrange can be readily used in currently available high-throughput instrumentation such as fluorescence microplate readers.

The numerous attributes of NanoOrange can be effectively used with those of CE to provide the clinical chemist with a valuable tool in clinical diagnosis: low protein concentration detection, nanolitre sample consumption, and short analysis times. The suitability of NanoOrange in clinical diagnostics is demonstrated here in the quantitation of human serum albumin (HSA). HSA is a clinically relevant protein used in the diagnosis of various disease states such as microalbuminuria, and has proven useful in drug binding studies [19–22]. Rapid 96-well fluorescence microplate and CE–LIF based assays for HSA are thus presented. NanoOrange performance in five commonly used buffers of various concentrations and pH is evaluated. Salt concentration effects, binding/fluorescence emission kinetics, and the ''stoichiometry'' of the HSA–NanoOrange complex formation are examined. The use of NanoOrange in biofluid profiling is demonstrated. To our knowledge this is the first time NanoOrange has been used in a CE–LIF format for the quantitation of nanomolar concentrations of a clinically relevant protein, and in biofluid profiling.

2. Experimental section

2.1. Apparatus

Microtitre plate assays were performed using Costar 96-well black flat bottom microplates (Corning, Acton, MA, USA) and a ''Victor^2'' fluorescence plate reader (EG&G Wallac, Ackron, OH, USA). All measurements were performed using a continuous lamp source energy of 9000 units and a 485 nm/535 nm filter set for excitation and emission, respectively. Fluorescence emission was measured in the normal aperture mode for 1.0 s at a measurement depth of 8 mm. Orbital shaking settings consisted of normal speed selection with an orbital diameter of 1.00 mm.

Capillary electrophoresis with laser-induced fluorescence was performed using a Crystal 310 Series CE system (ATI-Unicam, Mississauga, ON, Canada) equipped with a 48 position Peltier-cooled autosampler. Analyte detection was achieved using an in-house built system [16]. Briefly, the photomultiplier tube current was monitored via a current to voltage converter at 10 Hz using a National Instruments (Austin, TX, USA) NB-MIO-16-H (16 bit resolution) data acquisition board. All instrument settings were controlled by a LabView (National Instruments) application through the I/O port of the NB-MIO board. The 488 nm line from a 2 mW air-cooled Ar^+ laser (Ion Laser Technologies, Salt Lake City, UT, USA) was focused onto the capillary window using a 6.3 X focusing objective (Melles Griot, Irvine, CA, USA) with a numerical aperture of 0.2. System alignment was performed using a three-axis gimble mount (Newport, Irvine, CA, USA). Fluorescence emission was collected at right angles

to the excitation beam using a 16× microscope objective with a numerical aperture of 0.32 and working distance of 3.7 mm (Melles Griot), spatially filtered through a 800 μm pinhole, then spectrally filtered sequentially by a longpass 515EFLP and 580DF30 bandpass filter (Omega Optical, Brattleboro, VT, USA). The photons produced by the fluorophore were detected using a multi-alkali photocathode photomultiplier tube (R1477, Hamamatsu, Middlesex, NJ, USA) powered by a HC123-01, Hamamatsu high voltage power supply with an output range of −300 to −1100 volts. Unless otherwise indicated, the photomultiplier tube was operated at −700 V. The photocurrent was passed through a current-to-voltage converter and lowpass filter (10 MΩ resistor, 0.1 μF capacitor) and digitized at 10 Hz using the data acquisition system previously described. The collection objective and photomultiplier tube were fixed to a light-proof box containing the pinhole and filters. The data obtained was graphically illustrated using Igor Pro (Wavemetrics, Lake Oswego, OR, USA). CE experiments with absorbance detection were performed using previously described instrumentation [13].

Fluorescence excitation and emission spectra were obtained using an SLM-Aminco-Bowman spectrofluorimeter (Spectronic Unicam, Rochester, NY, USA). All measurements were performed at 25°C with a continuous 150 W Xenon lamp, scan rate of 2 nm/s, and photomultiplier tube setting of 700 V. Excitation spectra from 350 to 550 nm were obtained using an emission monochromator setting of 580 nm bandpass of 4 nm, whereas emission spectra from 500 to 700 nm were obtained with an excitation monochromator setting of 488 nm bandpass of 4 nm.

2.2. Reagents

All buffer reagents as well as HSA were purchased from Sigma (Mississauga, ON, Canada). NanoOrange dye was obtained as part of a NanoOrange Quantitation Kit (Molecular Probes, Eugene, OR, USA). CE–LIF separations were performed using 186 μm O.D., 50 μm I.D., 60 cm total length, 45 cm effective length bare-fused-silica capillaries (Polymicro Technologies, Phoenix, AZ, USA). Nanopure water with a conductivity of 18.3 MΩ cm^{-1} (Barnstead, Boston, MA, USA) was used for all buffer and dye solution preparations.

2.3. Procedures

2.3.1. Buffer concentration and pH studies

These were performed in 96-well microtitre plate wells by adding reagents in the following order: buffer, water, HSA and 10× NanoOrange. The HSA (1 mg/ml) and NanoOrange stock solutions (10×) were prepared fresh daily using nanopure water. NanoOrange was purchased initially as a 500× concentrate which was diluted 50-fold in water immediately prior to use in the above studies. Each well of the microtitre plate contained 130 μl of buffer, 20 μl of water, 20 μl of 10× NanoOrange, and 30 μl of 1 mg/ml HSA, for a total assay volume of 200 μl. All assays consisted of simultaneously loading eight wells with identical samples using a multichannel pipettor. Measurements were performed immediately following HSA addition and at 1 min intervals for 5 min with orbital shaking between readings.

2.3.2. NanoOrange fluorescence with varying HSA concentration studies

These utilized a similar approach to the above. In brief, HSA concentrations of 0, 10, 15, 20 and 25 μg/ml were examined at 1-min time intervals over a 30-min period, using an optimized assay buffer consisting of 15 m*M* borate (pH 9.0).

2.3.3. Effect of salt concentration on fluorescence emission

This was monitored by preparing 15 m*M* borate (pH 9.0) solutions containing 20 μg/ml HSA and 0–100 m*M* NaCl. Fluorescence emission was measured immediately and after 1 min of orbital shaking.

2.3.4. Optimization of NanoOrange concentration

Titration of HSA with NanoOrange was performed so as to take into account the time dependency of fluorescence emission. A stock solution of 10× NanoOrange was prepared in 15 m*M* borate (pH 9.0). Various volumes of this stock were added to wells containing 15 m*M* borate (pH 9.0) and

15 μg/ml HSA to obtain the desired final dye concentrations. The total volume of all wells was 200 μl. The fluorescence emission at a particular dye concentration was measured after 1 min of orbital shaking, followed by preparation and measurement of the next dye concentration.

2.3.5. Ninety-six-well microplate HSA calibration curve

A microtitre plate calibration curve for HSA was constructed as follows. Various HSA concentrations ranging from 1.67 μ*M* to 1.67 n*M* were prepared by performing serial dilutions of a 1 mg/ml HSA stock in 15 m*M* borate (pH 9.0). Eight wells were filled with 180 μl of a particular HSA concentration, followed by addition of 20 μl of 10× NanoOrange. Measurements were performed as described above.

2.3.6. CE–LIF NanoOrange HSA analysis

CE–LIF analyses were performed using the following procedure: HSA samples were injected at 100 mbar for 0.1 min, followed by a 0.01 min capillary tip/electrode rinse in buffer. Electrophoretic separations were performed by applying a potential of 30 kV (i.e. 500 V/cm). The capillary was conditioned with 0.1 *M* NaOH (1 bar for 30 s) followed by NanoOrange run buffer (1 bar for 60 s) between runs. The NanoOrange run buffer was prepared fresh by performing a 250-fold dilution of 500× dye stock in 15 m*M* borate (pH 9.0). It was deemed necessary to adequately filter the borate buffer using a Millipore Millex-LCR hydrophilic PTFE 0.45-μm syringe filter to avoid particulate scatter during the CE run. It should be noted that NanoOrange should be added to the filtered buffer but not prior to filtration, since dye retention by both nylon and hydrophilic PTFE membranes was observed.

CE–LIF calibration curves for HSA were constructed using similar HSA concentrations as for the microplate approach, but in this case NanoOrange was not added to the HSA solutions prior to analysis. HSA solutions were directly injected into the capillary and labeled on-column by incorporating NanoOrange in the run buffer. All HSA solutions were kept on ice between analyses.

3. Results and discussion

3.1. NanoOrange fluorescence excitation and emission spectra

The spectral characteristics of NanoOrange in the absence and presence of HSA were examined in order to determine the spectral filtering requirements of the assay. Fig. 1 illustrates the excitation and emission spectra obtained upon HSA binding. In the presence of HSA, $\lambda_{em,\ max}$ is blue-shifted by 24 nm from 604 to 580 nm. This shift was not accompanied by a corresponding shift in $\lambda_{ex,\ max}$ (data not shown). The large Stoke's shift, of approximately 100 nm, allows for efficient spectral discrimination between excitation light and fluorescence emission. Furthermore, a significant enhancement in fluorescence emission (i.e., ten-fold) is produced in the presence of 10 μg/ml HSA. NanoOrange's large emission band allows one the flexibility to utilize commonly used filters (e.g., fluorescein or tetramethyl-

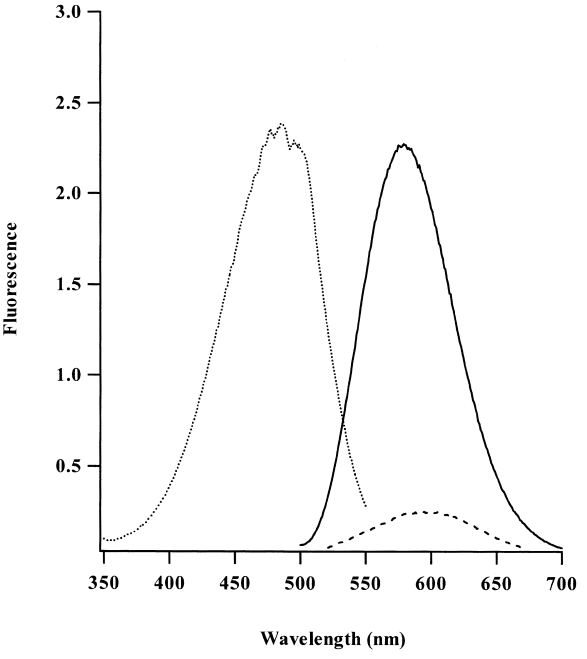

Fig. 1. Fluorescence excitation and emission spectra for 1× NanoOrange reagent±10 μg/ml HSA in water at 25°C. Excitation spectrum (. . . . .), emission spectrum in the absence of HSA (----), and emission spectrum (–) in the presence of HSA.

rhodamine-based emission filters), while still obtaining nanomolar protein detection limits.

3.2. NanoOrange buffer species, concentration, pH study

Five different buffers were chosen to cover a variety of useful pH ranges which are typically encountered in bioanalysis. The goal of this study was to characterize the effect of varying buffer species, concentration and pH on NanoOrange fluorescence emission upon protein binding. The following buffers were chosen for study: Tris–HCl, acetate, citrate, phosphate and borate. Recognized for its utility as a disease marker in various biofluid analyses, HSA was chosen as a model protein for this buffer study.

Two buffer systems were selected for evaluating the performance of NanoOrange under acidic conditions. Acetate has a useful pH range of about 3.5–5.5 which closely matches that of another commonly used buffer, citrate, which has a useful pH range of 3.0–5.0. A comparison of the effects of acetate and citrate on NanoOrange fluorescence emission is illustrated in Fig. 2. At low concentrations of both citrate and acetate (i.e., 6.5 m*M*, 15 m*M*), a trend of increased fluorescence emission with increasing pH was observed. This may be attributed to more favourable dye binding conditions as target residues of HSA and/or various NanoOrange functional groups are ionized. Due to the proprietary nature of this dye, no structural information on NanoOrange is presently available for confirmation of the latter. Increasing the buffer concentration to 32.5 m*M* disrupted this trend. Fluorescence emission decreased to a level equivalent to that observed for the middle of the useful pH range. Furthermore, a significant decrease in inter-well signal reproducibility (from 10 to 30%) was noted for these acidic buffers when the buffer concentration was increased from 6.5 to 32.5 m*M*. These effects are believed to be due in part, to a destabilizing effect on dye binding, caused by increasing salt concentration. In both buffer systems the counter ion was Na^+. This was examined in more detail in the salt concentration study described below. For both acetate and citrate buffers there was

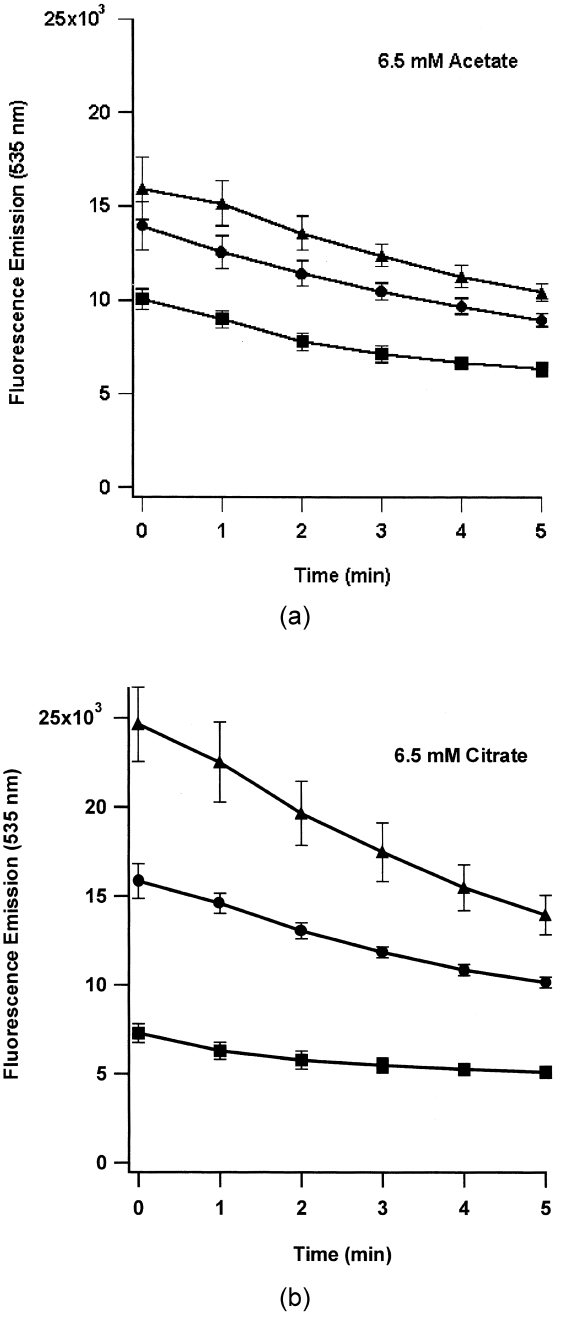

Fig. 2. A comparison of the effects of acidic buffers on 1× NanoOrange fluorescence emission over time, in the presence of 15 μg/ml HSA. Panel A: 6.5 m*M* acetate at pH 3.5 (■), pH 4.5 (●), pH 5.5 (▲). Panel B: 6.5 m*M* citrate at pH 3.0 (■), pH 4.0 (●), pH 5.0 (▲). Similar results to those shown were obtained for 15 m*M*, 32.5 m*M* acetate and citrate (data not shown). Error bars represent ±1 SD for eight replicate measurements.

a gradual decrease in fluorescence emission ranging from 10 to 30% over a 5-min incubation period. Since this trend was observed for all buffer systems examined, a proposed NanoOrange binding model is discussed in the binding kinetics section below.

In order to examine NanoOrange performance under neutral and basic conditions, three buffers with overlapping pH ranges were selected: phosphate (pH 6.0–8.0), Tris–HCl (pH 7.0–9.0), and borate (pH 7.0–9.0). A comparison of the effects of phosphate, Tris–HCl, and borate concentrations on NanoOrange fluorescence emission is illustrated in Fig. 3. In the case of phosphate, significant deviations from the trends established by the other buffers were observed. At 6.5 m*M* phosphate, increased stability in fluorescence emission over time resulted in higher emission intensity at pH 6.0 than at pH 7.0 or 8.0. Though such signal stability is highly desirable, the low fluorescence emission observed at pH 6.0 was considered suboptimal for achieving nanomolar HSA detection limits. Increasing the phosphate concentration to 15 m*M* (pH 6.0) resulted in a four to five-fold enhancement in signal intensity with a corresponding loss in fluorescence stability (10% min^{-1}). Interestingly, further augmenting the concentration to 32.5 m*M* decreased the fluorescence emission at pH 7.0 and 8.0 by 30–40%, while maintaining signal intensity at pH 6.0. In terms of the binding model proposed below, it appears that at pH 6.0, and low phosphate concentration (i.e., 6.5 m*M*), relatively few NanoOrange molecules can stack onto the HSA surface. This may be due to repulsive effects between dye molecules. The inability to stack onto the surface of HSA thus manifests itself in reduced signal intensity and increased stability. Increasing the phosphate ion concentration is thought to enhance fluorescence emission by shielding the proposed ionized groups on NanoOrange, hence promoting dye stacking. However, since Na^+ is correspondingly increased in concentration, one cannot arbitrarily increase phosphate concentrations with the hopes of boosting signal intensity.

Tris–HCl did not manifest all of the same trends as for phosphate (Fig. 3). Similar to the acidic buffer study, Tris–HCl exhibited a trend of increased fluorescence emission with increasing pH for all concentrations tested. In comparison to the phosphate study, increasing Tris–HCl concentration had a similar effect, augmenting emission intensity by 2–3.5–fold. In this case, Cl^- ions may be playing a similar role to phosphate ions in providing a charge shielding effect.

In comparison to Tris–HCl and phosphate, 6.5 m*M* borate provided higher fluorescence emission at the pH values examined, and exhibited the same trend between pH and signal intensity as Tris–HCl. Once again, emission was enhanced approximately 50% by increasing buffer concentration to 15 m*M*. Use of 32.5 m*M* borate did not result in significantly improved fluorescence emission.

Thus, there is a certain degree of flexibility in buffer selection for use with NanoOrange. In general, acidic buffers such as citrate and acetate are not recommended due to inferior fluorescence emission. Phosphate, Tris–HCl, and borate are all acceptable choices, with a preference for concentrations in the 15–32.5 m*M* concentration range. Of the five buffers examined, 30 m*M* Tris–HCl (pH 9.0), 15 m*M* phosphate (pH 9.0), 15 m*M* borate (pH 9.0), and 32.5 m*M* borate (pH 9.0) were the best candidates for use in a HSA assay. The pH optimum of these various buffers (i.e., pH 9.0) was well suited to a CE-based HSA assay since protein adsorption to the capillary wall is significantly reduced at high pH [23]. The buffer selected for further studies consisted of 15 m*M* borate (pH 9.0). Borate has been successfully used in CE-based biofluid analysis and the well-documented effectiveness of this buffer system was considered more important than a ca. 1.5-fold increase in fluorescence emission one would obtain using Tris–HCl. Use of borate was favored over phosphate due to current generation/joule heating issues which could require a lower separation potential hence longer analysis times. Fluorescence emission was only marginally higher at 32.5 m*M* borate (pH 9.0) than 15 m*M* borate (pH 9.0) hence in an effort to minimize current generation during the separation, the latter was selected.

3.3. Salt concentration study

Since biofluids often contain relatively high salt concentrations, a study was performed to ascertain the impact of increasing salt concentration on NanoOrange fluorescence emission. Utilizing 15 m*M*

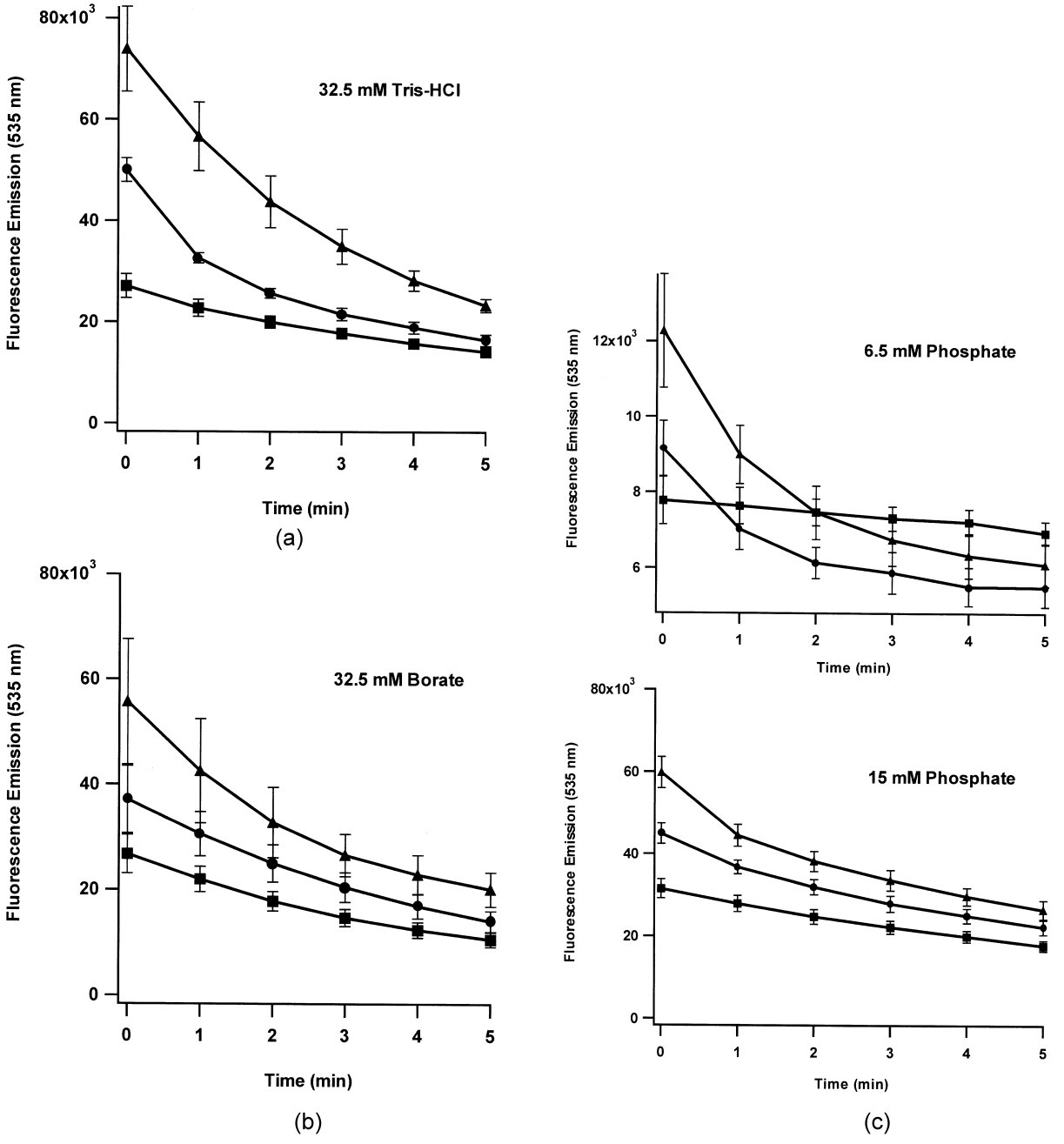

Fig. 3. A comparison of the effects of neutral and basic buffers on 1× NanoOrange fluorescence emission over time, in the presence of 15 μg/ml HSA. Panel A: 32.5 m*M* Tris–HCl at pH 7.0 (■), pH 8.0 (●), pH 9.0 (▲). Panel B: 32.5 m*M* borate at pH 7.0 (■), pH 8.0 (●), pH 9.0 (▲). Panel C: 6.5 m*M* phosphate and 15 m*M* phosphate, at pH 6.0 (■), pH 7.0 (●), pH 8.0 (▲). Similar results to those shown were obtained for 6.5 m*M*, 15 m*M* Tris–HCl and borate (data not shown). Error bars represent ±1 SD for eight replicate measurements.

borate (pH 9.0), NaCl concentrations ranging from 0 to 100 m*M* were added to the assay buffer. Increasing the concentration of NaCl had a detrimental effect on fluorescence emission. After as little as 1 min of incubation, NanoOrange fluorescence intensity decreased by approximately 13% in the absence of NaCl as opposed to a relatively consistent decrease of 25% in the presence of NaCl. Furthermore, after 1 min of incubation, a plateau region from 20 to 80 m*M* NaCl was observed, over which fluorescence emission declined marginally by 5%. Two significant drops of 30 and 20% were observed on either side of this plateau as the NaCl concentration was increased from 0 to 20 m*M* and 80 to 100 m*M*, respectively. The data suggests that in the presence of NaCl, optimal fluorescence emission is attained by prediluting biofluid samples so as to diminish salt concentration to a level ranging from 20 to 80 m*M*. Combined with the effects of increasing buffer concentration on fluorescence emission, it appears as though NanoOrange fluorescence is related to several factors which include counter-anion stabilization and Na^+ destabilization. By analogy, recent crystallographic and energetic analyses of binding of selected anions to the yellow variants of Green Fluorescent Protein has indicated anion binding effects on fluorescence emission [24].

3.4. NanoOrange binding and fluorescence emission kinetics

The fluorescence stability of non-covalent dyes under aqueous conditions is often a key parameter for successful protein labeling. Indeed, dye stability was an issue in a previous CE–LIF based HSA assay which utilized the tricarbocyanine dye Indocyanine Green [17]. NanoOrange-protein complexes are stable for at least 6 h when diluted in a detergent-based 1× quantitation diluent (provided in the NanoOrange quantitation kit). However, the present study utilized a modification of this protocol which does not utilize detergent. An examination of NanoOrange fluorescence emission versus time revealed that fluorescence enhancement upon binding is rapid. Maximal fluorescence emission essentially occurs in the time required to add HSA to a microtitre plate and place it in the instrument. The fluorescence emission of NanoOrange–HSA complexes decreases over time. The fluorescence decay curves (see Fig. 4) for various HSA concentrations indicate that fluorescence emission follows zero order kinetics with respect to protein concentration. In the absence of HSA, unbound NanoOrange fluorescence emission is relatively stable.

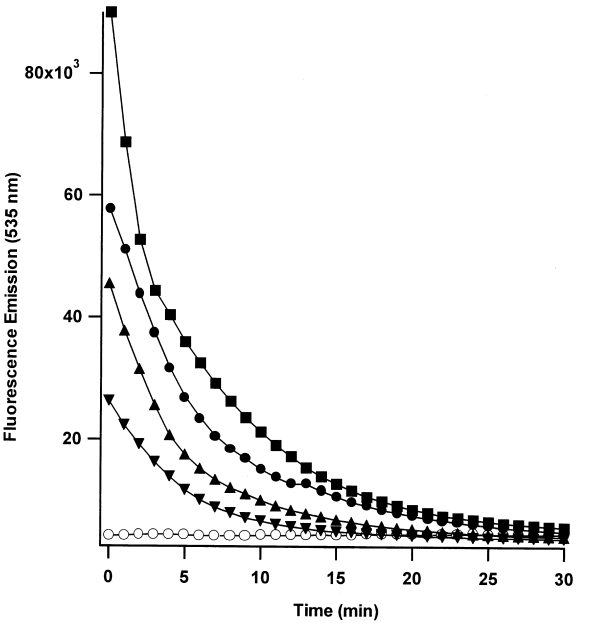

Fig. 4. Fluorescence emission decay curves for 1× NanoOrange in the presence of various HSA concentrations in 15 m*M* borate (pH 9.0): 25 μg/ml (■), 20 μg/ml (●), 15 μg/ml (▲), 10 μg/ml (▼), 0 μg/ml HSA (○). SD for all data points (eight replicate measurements) = ±10%.

In order to explain this rapid decay in fluorescence emission, a NanoOrange binding model is proposed. NanoOrange molecules are believed to rapidly bind to the surface of HSA, producing maximal fluorescence emission. These dye molecules in turn serve as ''nucleation'' sites for further dye binding. This slower process of NanoOrange accumulation results in fluorescence self-quenching. The self-quenching capability of dye molecules in close proximity to one another is in fact used extensively in fluorescence-based phospholipase detection methods [25]. In the manufacturer's NanoOrange labeling method, heating in the presence of a detergent solution for 10 min is followed by a 20-min cooling period prior to analysis. The above quenching effect, as shown in Fig. 4, may not be observed in the manufacturer's method, since after 30 min fluorescence intensity is

such that HSA concentrations as low as 10 ng/ml can still be detected.

This has implications in the design of a NanoOrange HSA assay, with highest sensitivity obtained at short incubation times (i.e., 1 min). Contrary to many detection schemes which require several minutes to several hours of incubation for maximal signal generation, the use of NanoOrange has a requirement for analysis within only a few minutes of protein addition. The high-throughput nature of this assay is thus highly attractive.

3.5. HSA titration with NanoOrange

The development of cost-effective assays capable of detecting nanomolar protein concentrations is of significant value to the clinical laboratory. It was thus necessary to determine the optimal amount of NanoOrange to include in the assay buffer. A titration of 15 μg/ml HSA with NanoOrange concentrations ranging from 0–4× was performed (Fig. 5). A saturable binding curve was obtained, there appears to be no advantage to using more than 1× NanoOrange. Use of 1.5–2× NanoOrange did not produce a change in the signal-to-background ratio. However, dye concentrations of 2.5× and higher resulted in decreased fluorescence emission. Quenching and the inner filter effect are believed to play an increasingly important role at these elevated concentrations, resulting in reduced signal intensity. It should be noted that the conventional detergent-based NanoOrange protocol also recommends the use of 1× NanoOrange. Since NanoOrange is provided as a 500× concentrate, it is not possible to express binding stoichiometry in terms of a mole fraction. It is likely, however, that many different complexes are formed from the addition of dye to HSA, especially in light of the binding model proposed above. A 1× NanoOrange concentration was thus used for the microplate assay described below.

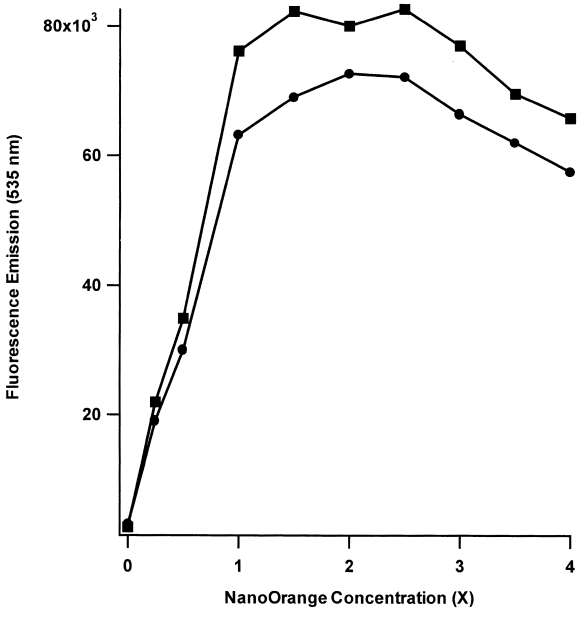

Fig. 5. Titration of 15 μg/ml HSA with NanoOrange concentrations ranging from 0 to 4×. Measurements performed in 15 m*M* borate (pH 9.0) at $t=0$ min (■) and $t=1$ min (●). SD for all data points (eight replicate measurements)=±10%.

3.6. Ninety-six-well microtitre plate assay for HSA

A 96-well microtitre plate assay was developed for the sensitive detection of HSA. A HSA calibration curve was constructed ($N=8$). This curve consisted of two distinct linear regions: 91 n*M* to 1.47 μ*M*, and 1.47 to 46 n*M* HSA. The assay may thus be performed for HSA concentrations which span three orders of magnitude by selecting the appropriate linear portion from the calibration curve. The calibration curve resembles that observed in the presence of detergent [18]. A signal-to-background noise ratio of nine was obtained for 1.47 n*M* HSA. It should be noted that a 535 nm emission filter was utilized in this assay, an emission filter centered at 580 nm would be expected to produce lower detection limits. The intra-assay precision for this microplate assay ranged from 10.5 to 7.8% for 1.47 n*M* and 1.47 μ*M* HSA, respectively. The use of black microplates is highly recommended due to the high background obtained with clear bottom plates. Due to the fluorescence emission decay rate previously discussed, it is beneficial to utilize a multichannel pipettor or suitable rapid automated well dispensing unit.

3.7. CE–LIF HSA quantitation

A CE–LIF based assay which utilizes NanoOrange as an on-column labeling reagent was developed. A small sample plug is injected into the

capillary, analytes are separated and labeled with NanoOrange as they migrate electrophoretically through a run buffer containing the fluorogenic dye, followed by on-column detection. This ability to derivatize analytes on-column confers several notable advantages. Contrary to off-column derivatization schemes in which labeled samples are consumed/dedicated to a particular analysis, the NanoOrange CE–LIF assay described below ensures sample vials never come into contact with dye. Furthermore, automated sample injection systems typically require 10 μl sample volumes for injection. These features are particularly useful in cases where a limited amount of sample is available, or cost restrictions result in reduced sample accessibility. Since only nanolitre sample volumes are injected onto the capillary, one can essentially preserve the initial sample for later use in performing other analyses such as mass spectrometry and ELISA.

CE–LIF calibration curves for HSA ($N=3$) were determined as shown in Fig. 6. Individual curves exhibited relative linearity ($R=0.99$) from 3.2 n*M* to 0.82 μ*M*. However, a gradual decrease in assay sensitivity over time was observed. The time required to construct each curve was approximately 1 h, such that the third curve was obtained at least 3 h following initial preparation of the NanoOrange run buffer. At HSA concentrations below 0.4 μ*M*, calibration curves constructed within the first 2 h of run buffer preparation possess very similar sensitivities. Longer time periods (i.e., 3 h) tended to be associated with significantly lower calibration curve sensitivity. This was attributed to increased dye instability in aqueous conditions. The lifetime of NanoOrange thus appeared to be reduced, ca. threefold, when not diluted in the standard detergent solution provided in the kit. As such, periodic calibration and/or standardization would be required, the internal standardization method may also be particularly effective in this case.

A key feature of the assay is the ability to efficiently label HSA as it migrates through the capillary. Contrary to the microplate scenario, the HSA sample plug is initially devoid of NanoOrange, and is flanked on both sides with run buffer containing NanoOrange. Labeling efficiency thus depended on the analyte's ability to migrate into the adjacent NanoOrange zone or the dye's ability to

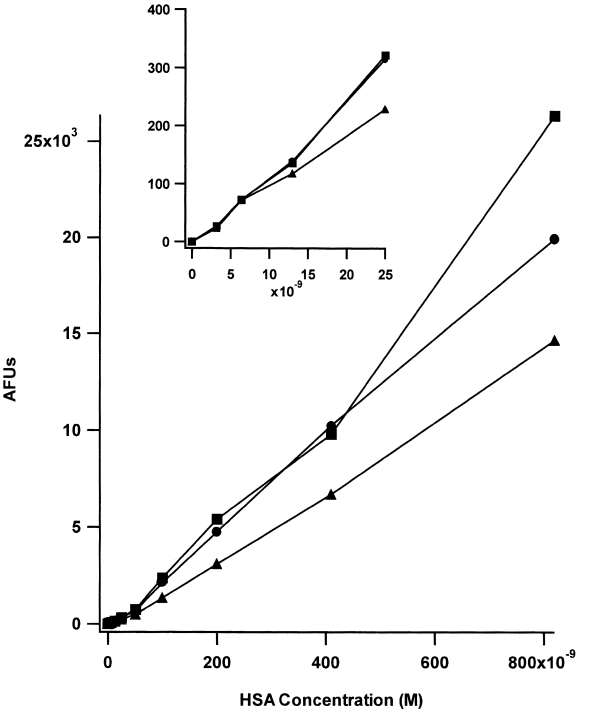

Fig. 6. CE–LIF calibration curves for HSA utilizing 2× NanoOrange in the run buffer. Conditions: 60 cm, 186 μm O.D., 50 μm I.D., bare-fused-silica capillary; 15 m*M* borate, (pH 9.0)/2× NanoOrange run buffer, 0.6 bar/s injection, 500 V/cm separation potential; LIF detection (arbitrary fluorescence units – AFUs representing peak height). Calibration curves at $t=1$ (■), $t=2$ (●), and $t=3$ h (▲) after buffer preparation. Inset shows linear portion ($R=0.99$) for HSA concentrations in the nanomolar range.

overtake the sample plug within a short period of time. This electrophoretic mixing process, as opposed to microplate orbital shaking, resulted in different optimal dye concentrations. It was determined that incorporation of 2× NanoOrange in the run buffer enhanced the signal-to-noise ratio by approximately a factor of two (results not shown). A signal-to-noise ratio of 5.6 was obtained for 3.2 n*M* HSA. It is important to note that this corresponds to actually labeling 3.2 n*M* HSA and not simply labeling at high protein concentration followed by serial dilutions typical of other labeling methods. For comparative purposes, an instrumental limit of detection of 0.1 n*M* was obtained for fluorescein alone (no HSA) using the same experimental parameters,

replacing the 580df30 filter with a 535df55 filter. In the interest of developing a low cost assay, concentrations of greater than 2× were not examined, though these could feasibly result in improved detection limits. According to the proposed NanoOrange binding model, dye–protein complexation is followed by self-quenching over time. In the present assay format, HSA–NanoOrange complex migration times of approximately 3 min are attained. Improved detection limits can therefore be expected with shorter analysis times (i.e., shorter effective capillary lengths).

The advantages of utilizing NanoOrange in biofluid analysis are illustrated in Fig. 7. On-column labeling of human serum with NanoOrange enhances the signal-to-background ratio of all components by up to two orders of magnitude. This essentially allows one to detect lower concentrations of biofluid protein components than in absorbance detection schemes. Furthermore, the profile obtained using NanoOrange and LIF shows similarities to that observed in the absence of dye with absorbance detection. Systematic improvements in resolution were observed by lowering the electric field in the case of NanoOrange labeling to 250 V/cm, as shown in Fig. 7. Significant improvements were not observed at electric fields below 250 V/cm (data not shown). Addition of NanoOrange to the serum significantly enhanced the signal observed for some zones but may have also altered the electrophoretic mobilities making direct comparisons to the absorbance literature problematic. Positive identification of the sample zones has not yet been accomplished and will be the focus of future work.

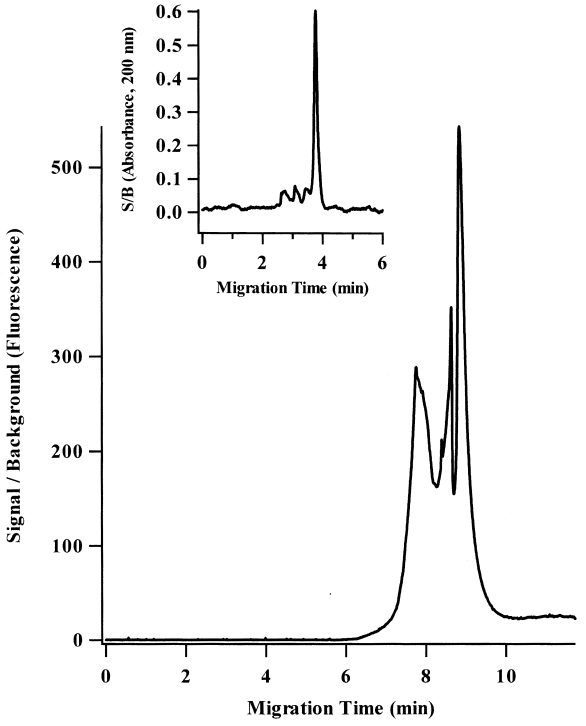

Fig. 7. CE–LIF electropherogram of 60× diluted human serum utilizing 1× NanoOrange in the run buffer. Conditions: 60 cm total length, 45 cm effective length, 186 μm O.D., 50 μm I.D., bare-fused-silica capillary; 20 m*M* borate, (pH 9.25)/1× NanoOrange run buffer, 0.6 bar/s injection, 250 V/cm separation potential; spectral filters=515 EFLP/535df55, PMT=− 0.900 kV. Inset illustrates human serum profile obtained using a 60 cm total length, 45 cm effective length, 350 μm O.D., 50 μm I.D., bare-fused-silica capillary; 20 m*M* borate, (pH 9.25) run buffer, 5 cm/60 s hydrodynamic injection, 417 V/cm separation potential and absorbance detection.

4. Conclusion

The numerous attributes of NanoOrange have been effectively coupled with those of CE to provide the clinical chemist with a valuable tool in clinical diagnosis: low protein concentration detection, nanolitre sample consumption, and short analysis times. To our knowledge, this is the first time that the non-covalent fluorogenic dye, NanoOrange, has been used for the on-column labeling of a clinically significant protein in CZE–LIF, as well as for biofluid analysis.

The above approach incorporated NanoOrange in the run buffer to achieve dye–protein complex formation. In order to further reduce assay cost, a plug-plug on-column labeling strategy is currently being investigated. In this format, a plug of analyte is injected, followed by a nl plug of dye (or vice versa depending on their relative electrophoretic mobilities). We are currently examining the use of NanoOrange in a microchip format, as well as a CE–LIF based clinical biofluid analysis tool. Additional protocols are being evaluated in order to expand the scope of NanoOrange as a universal labeling reagent.

Acknowledgements

The authors are grateful to the Concordia University Functional Genomics Center for use of the Victor^2 fluorescence plate reader. The authors wish to acknowledge financial support provided by the Natural Sciences and Engineering Research Council of Canada (NSERC), Fonds pour la Formation de Chercheurs et l'Aide à la Recherche (FCAR), and David J. Azrieli.

References

[1] M.T. Kelly, H. Fabre, D. Perrett, Electrophoresis 21 (2000) 699.
[2] M.S. Liu, S. Rampal, D. Hsiang, F.T. Chen, Mol. Biotechnol. 15 (2000) 21.
[3] C. Petrini, M.G. Alessio, L. Scapellato, S. Brambilla, C. Franzini, Clin. Chem. Lab. Med. 37 (1999) 975.
[4] X. Bossuyt, G. Schiettekatte, A. Bogaerts, N. Blanckaert, Clin. Chem. 44 (1998) 749.
[5] I.H. Lee, D. Pinto, E.A. Arriaga, Z. Zhang, N.J. Dovichi, Anal. Chem. 70 (1998) 4546.
[6] M.J. Schmerr, A.L. Jenny, M.S. Bulgin, J.M. Miller, A.N. Hamir, R.C. Cutlip, K.R. Goodwin, J. Chromatogr. A 853 (1999) 207.
[7] G. Hunt, W. Nashabeh, Anal. Chem. 71 (1999) 2390.
[8] E.S. Yeung, J. Chromatogr. A 830 (1999) 243.
[9] J. Caslavska, D. Allemann, W. Thormann, J. Chromatogr. A 838 (1999) 197.
[10] I. German, R.T. Kennedy, J. Chromatogr. B. Biomed. Sci. Appl. 742 (2000) 353.
[11] S. McWhorter, S.A. Soper, Electrophoresis 21 (2000) 1267.
[12] T. Walz, J. Geisel, M. Bodis, J.P. Knapp, W. Herrmann, Electrophoresis 21 (2000) 375.
[13] P.R. Banks, D.M. Paquette, J. Chromatogr. A 693 (1995) 145.
[14] L. Reyderman, S. Stavchansky, Anal. Chem. 69 (1997) 3218.
[15] M.A. Marino, M. Devaney, P.A. Davis, J.E. Girard, J. Chromatogr. B. Biomed. Sci. Appl. 732 (1999) 365.
[16] M.D. Harvey, D. Bandilla, P.R. Banks, Electrophoresis 19 (1998) 2169.
[17] E.D. Moody, P.J. Viskari, C.L. Colyer, J. Chromatogr. B. Biomed. Sci. Appl. 729 (1999) 55.
[18] R.P. Haugland (Ed.), Handbook of Fluorescent Probes and Research Chemicals, 6th ed., Molecular Probes, Eugene, OR, 1996.
[19] L.M. Pedersen, P.G. Sorensen, Acta Oncol. 39 (2000) 145.
[20] J.S. Jensen, B. Feldt-Rasmussen, S. Strandgaard, M. Schroll, K. Borch-Johnsen, Hypertension 35 (2000) 898.
[21] M. Purcell, J.F. Neault, H.A. Tajmir-Riahi, Biochim. Biophys. Acta 1478 (2000) 61.
[22] A. Frostell-Karlsson, A. Remaeus, H. Roos, K. Andersson, P. Borg, M. Hamalainen, R. Karlsson, J. Med. Chem. 43 (2000) 1986.
[23] J.P. Landers (Ed.), Handbook of Capillary Electrophoresis, 2nd ed., CRC Press, Boca Raton, 1996.
[24] R.M. Wachter, D. Yarbrough, K. Kallio, S.J. Remington, J. Mol. Biol. 301 (2000) 157.
[25] T. Meshulam, H. Herscovitz, D. Casavant, J. Bernardo, R. Roman, R.P. Haugland, G.S. Strohmeier, R.D. Diamond, E.R. Simons, J. Biol. Chem. 267 (1992) 21465.